

Figure S1. Dynamic properties of plasma membrane recruitment of activated OS. A.

Immunofluorescence images of total SRC WT-GFP and its activation marker (PhosphoY416) show the high compartmentalization of activated SRC (PhosphoY416/SRC wt-GFP) in dynamic acto-adhesive structures, such as lamellipodia and the invadosome.

B. Representative time series of TIRF images of OS co-expressed with CIBN-GFP-Caax in response to local blue light stimulation. Transient stimulation induces a characteristic rapid (5 sec) and transient (after 300 sec) recruitment of OS to the plasma membrane (blue curve) in comparison with non-stimulated regions (black curve). Local stimulation of OS (co-expressed CIBN-GFP-Caax) presents a minimal spatial resolution of 5 μm around stimulation spot.

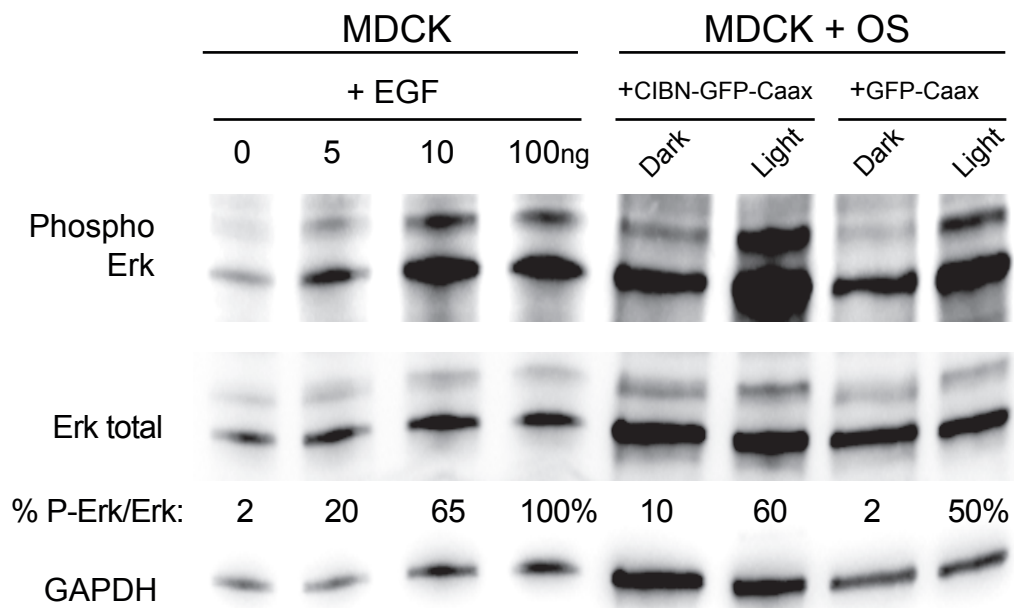
C. Expression of activated mutant SRCY527F-mCh induces dynamic dorsal ruffles (red arrow) in fibroblasts.

D. Evaluating the phospho-paxillin/paxillin ratio by western blot and its quantification (SD; N=3) shows the poor leakiness of non-stimulated OS in the dark (stably co-expressed with CIBN-GFP-Caax in MDCK cells) in comparison to MDCK not expressing OS.

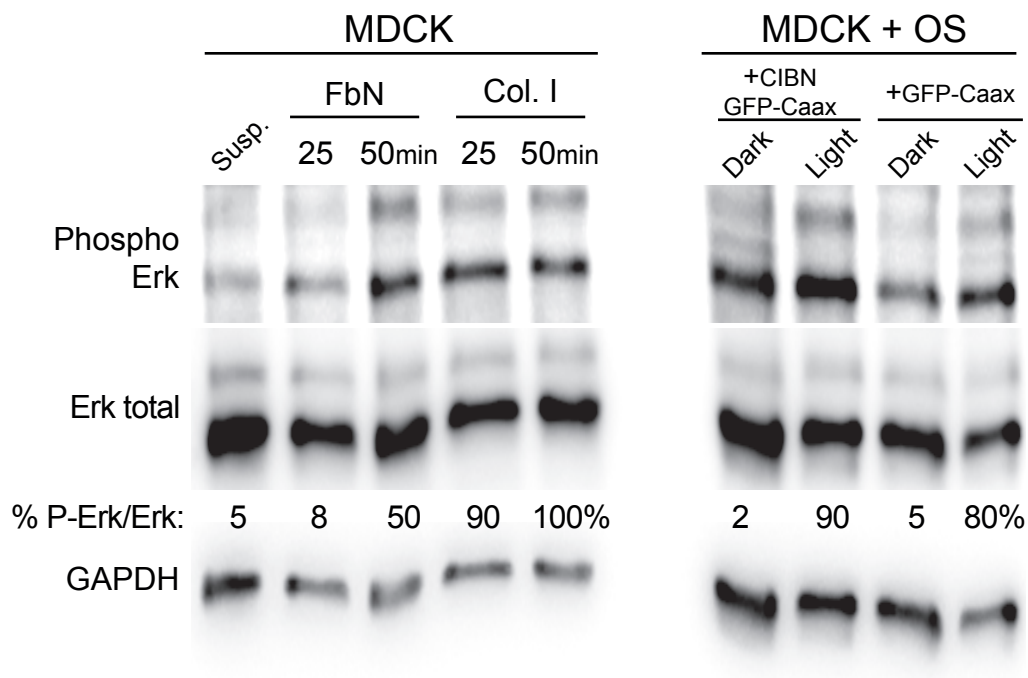
Scale bars: 1 μm (A), 5 μm (C).

Figure S2

A



B



C

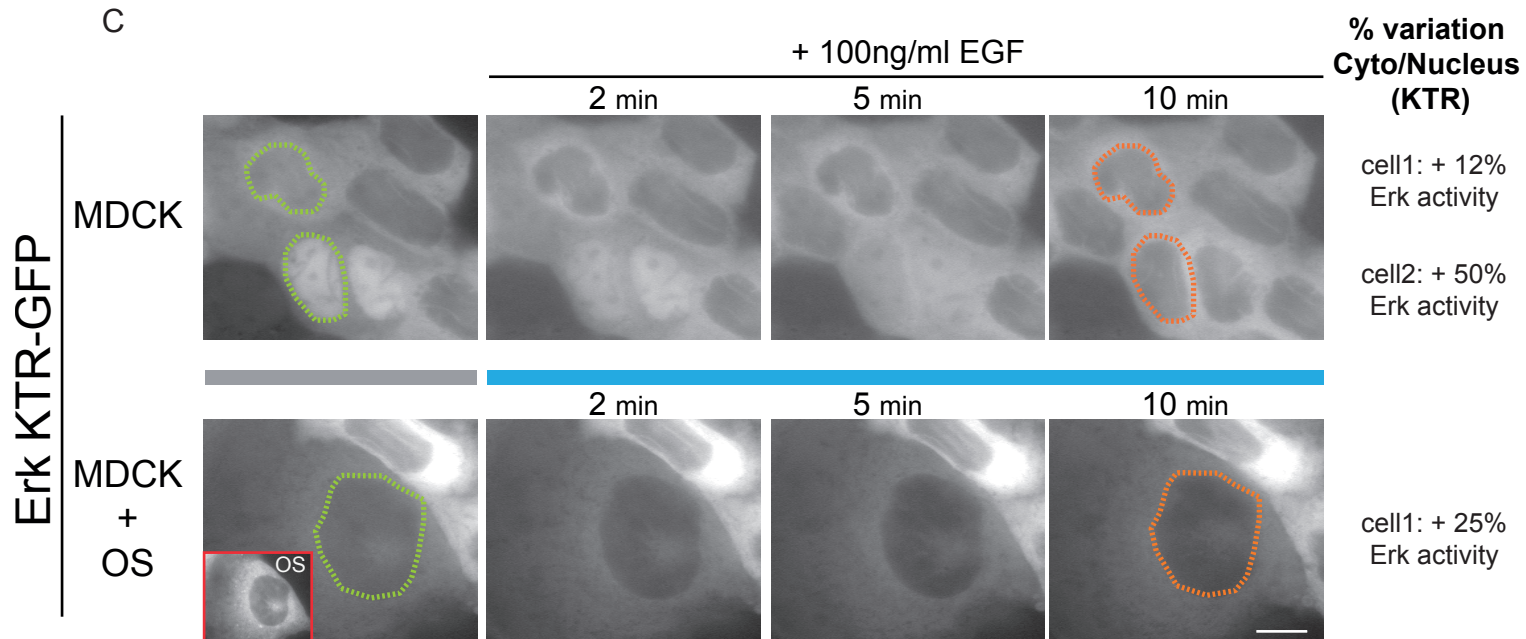


Figure S2. Different modes of OS activation activate ERK signaling pathways in the same range than physiological stimuli.

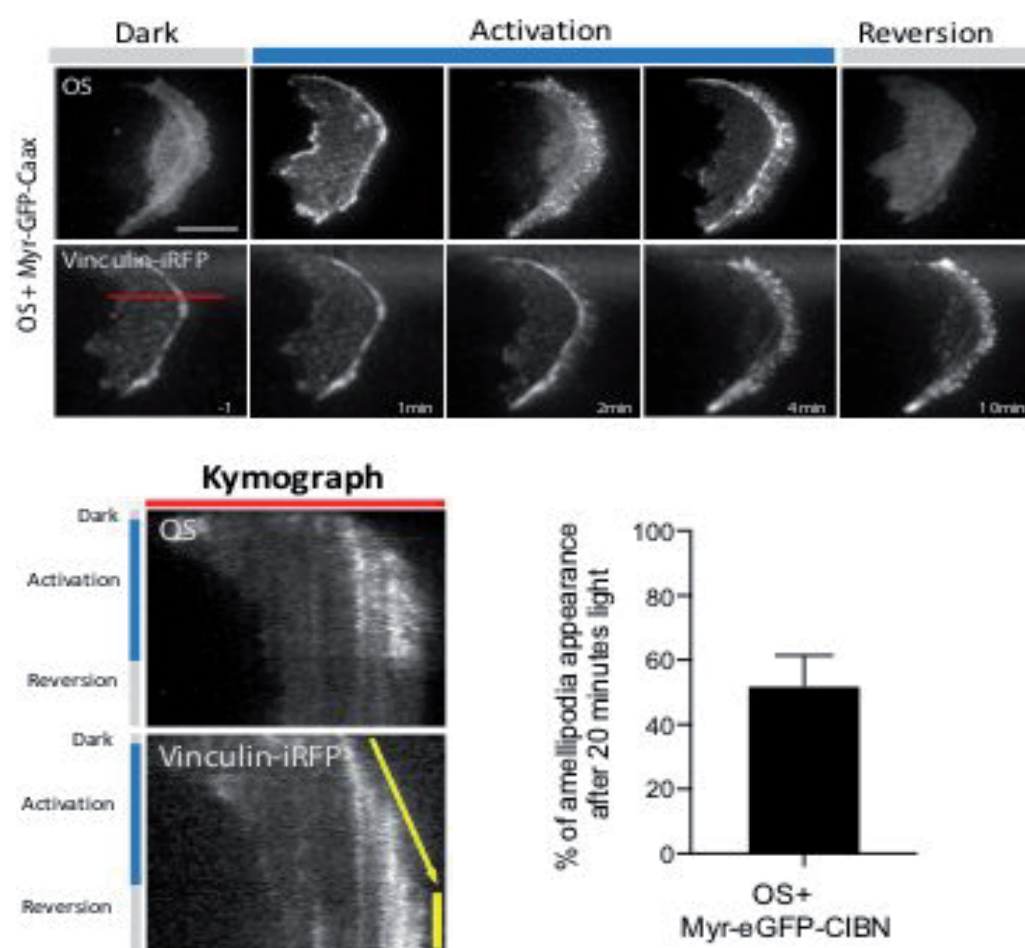
A. Evaluating the phospho-Erk/erk ratio by western blot (N=3) shows that 15min activation of OS with or without CIBN-GFP-Caax activates Erk phosphorylation of MDCK cells in the same range than 15min activation with croissant doses of EGF.

B. Evaluating the phospho-Erk/erk ratio by western blot (N=3) shows that 50min activation of OS with or without CIBN-GFP-Caax activates Erk phosphorylation of MDCK cells in the same range than MDCK spreading on either fibronectin (FbN) or collagen I (Col.I).

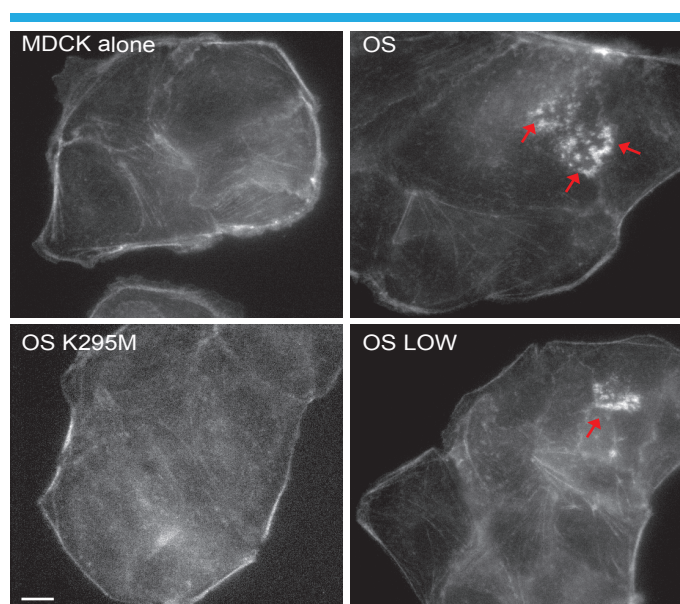
C. Representative fluorescence images of the Erk reporter, Erk-KTR-GFP, in response to either EGF treatment or OS activation. Both stimulation led to a rapid and comparable exclusion of Erk-KTR-GFP from the nucleus indicating the rapid specific phosphorylation of this probe by activated Erk in response to both treatments.

Scale bar: 2 μ m.

A



B



C

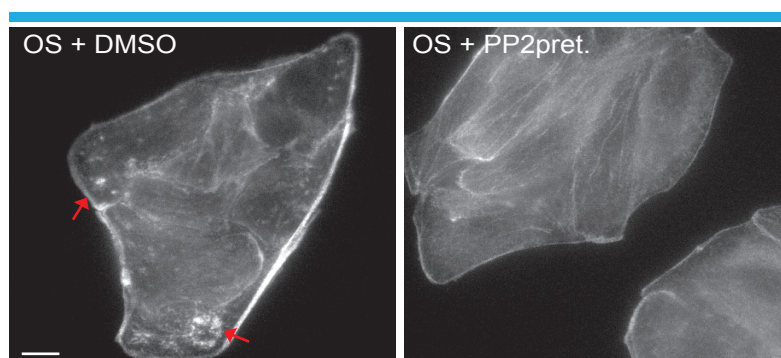


Figure S3. Perturbation of the kinase activity of OS affects invadosome formation. A.

Representative time serie illustrating that light-dependent myr-associated OS oligomers relocalize in adhesive sites and induce the formation of lamellipodia in MDCK cells (blue light 50ms pulse every 30s over 10 min). Kymograph analysis (on the red line) showed high dependency of the expansion lamellipodia to blue light (yellow arrow). The quantification of the percentage of cells forming lamellipodia after blue light stimulation of MDCK cells expressing both OS and Myr-CIBN-GFP (N=4; > 30 cells per condition).

B. Representative confocal images of invadosomes (phalloidin, red arrows) in MDCK stimulated with blue light for 15 minutes and expressing either nothing, OS, OS-K295M (kinase dead) or OS LOW.

C. Representative confocal images MDCK expressing OS and stimulated with blue light for 15 minutes. SRC inhibition by PP2 treatment abolished the formation of invadosomes (phalloidin, red arrow) in response to blue light.

Scale bar: 10 μ m.

Figure S4

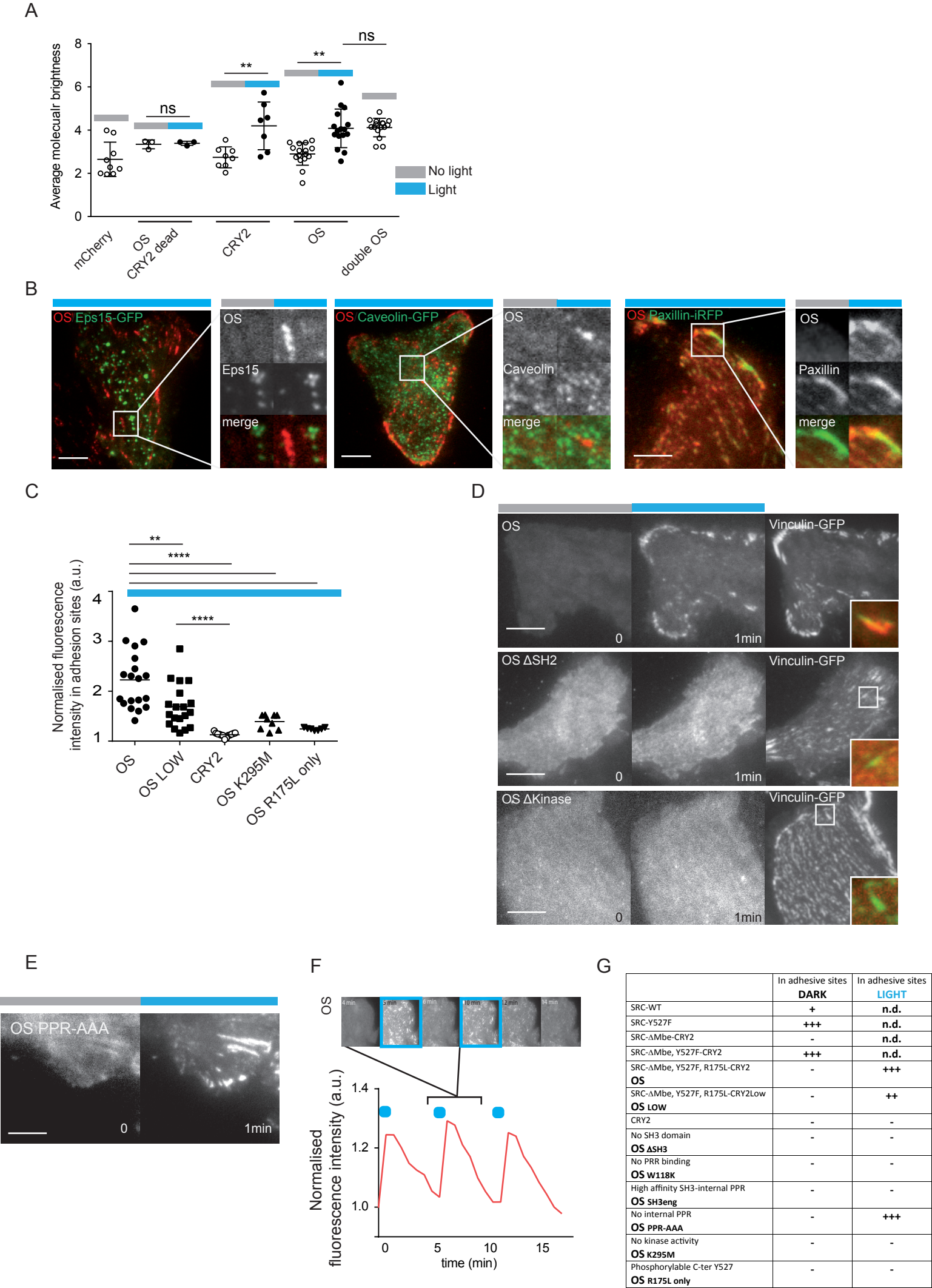


Figure S4. Characteristic of OS oligomers relocation in adhesive sites.

A. Quantification of the average molecular brightness revealed the oligomerization state of OS and OS mutants in response to photoactivation (SD; N=3; >15 cells per condition, unpaired t test).

B. Representative TIRF images of activated OS and different markers of subcellular structures, such as clathrin pits (EPS15-GFP), caveolae (caveolin1-GFP) or adhesive sites (paxillin-GFP).

C. Quantification of OS, OS LOW (CRY2 mutant presenting decreased oligomerization) and its kinase or C-ter mutants at the plasma membrane after blue TIRF photostimulation (SD; N=3; >30 cells per condition, unpaired t test).

D. Representative time series of TIRF images of OS mutants with the SH2 domain or kinase domain deleted and poorly relocated in adhesive sites (vinculin-iRFP) in response to blue TIRF photostimulation.

E. Representative time series of TIRF images of OS PRR-AAA mutants with a non-functional internal PRR that is relocated in characteristic adhesive sites in response to blue TIRF photostimulation.

F. Representative time series of TIRF images of OS dimer dynamics in response to blue TIRF photostimulation. Transient stimulation induces rapid and reversible recruitment of OS oligomers to adhesive sites.

G. Table summarizing the property of adhesive sites relocation of the different used mutants.

Scale bars: 2 μ m (B, E), 5 μ m (D).

Figure S5

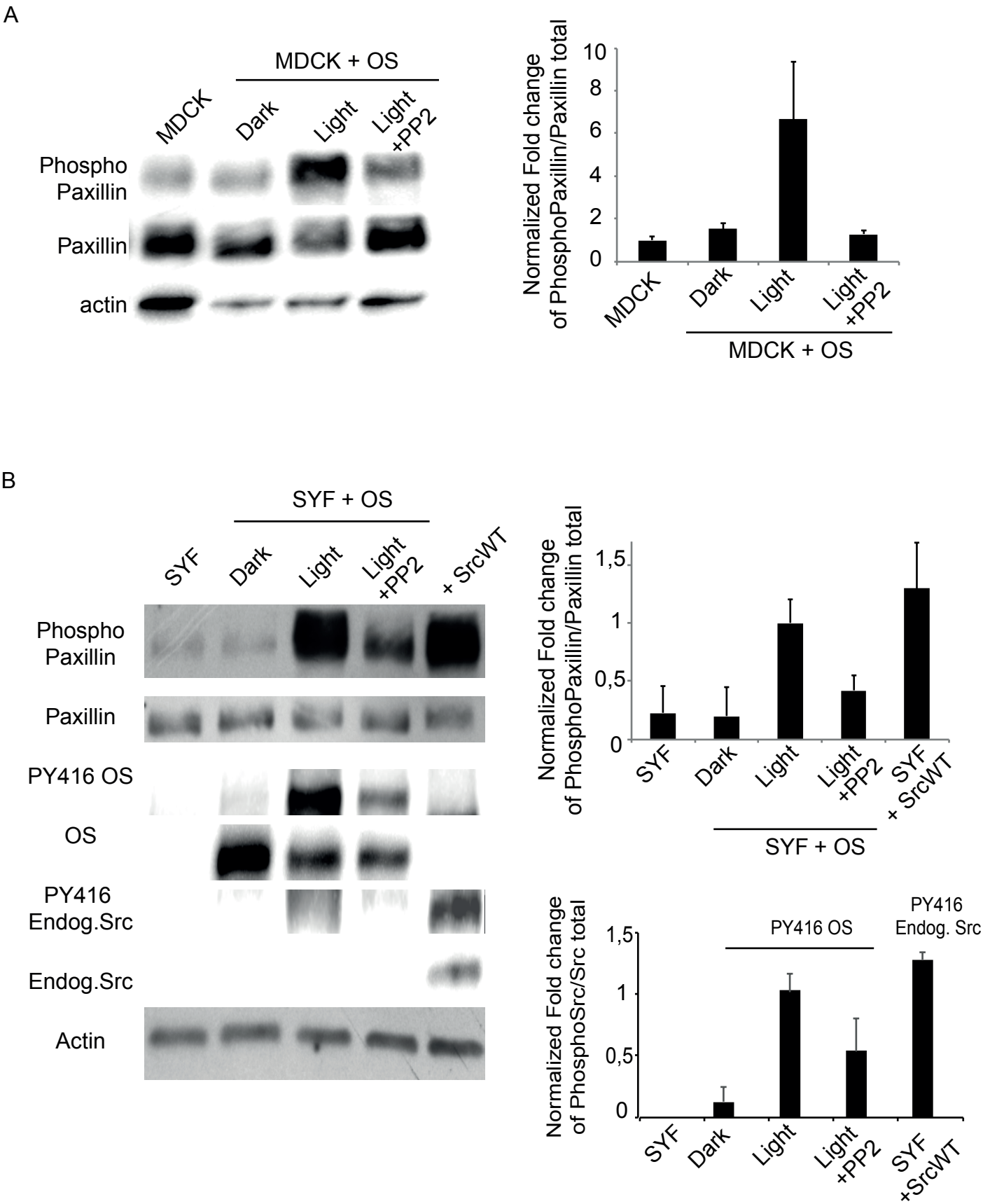


Figure S5. Evaluation of OS leakiness and the dynamic range response in different regimens of OS activation and cell types.

A. Evaluating phospho-paxillin/paxillin ratio by western blot and its quantification (SD; N=3) shows the poor leakiness of non-stimulated OS when expressed in MDCK cells and maintained in the dark, in comparison to MDCK not expressing OS.

B. Evaluating phospho-paxillin/paxillin and phospho-Y416 (OS or endogenous SRC)/(total OS or endogenous SRC) ratios by western blot and its quantification (SD; N=3) shows the poor leakiness of non-stimulated OS in the dark and expressed in SYF cells (SRC^{-/-} Yes^{-/-} Fyn^{-/-} cells). Light-dependent OS dimers induce the same dynamic range of paxillin phosphorylation and kinase activation as did re-expressing SRC WT in SYF cells.

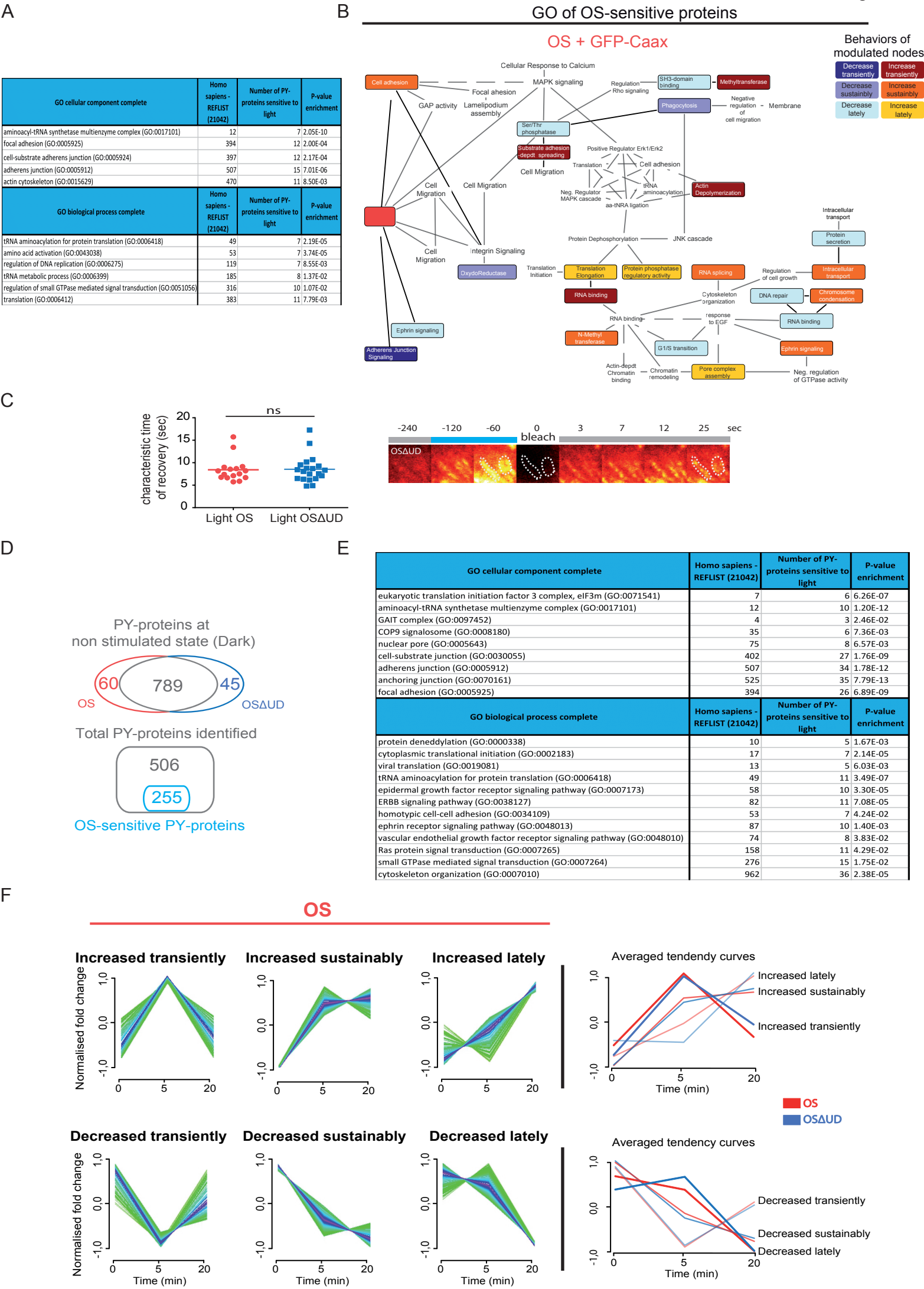


Figure S6. GO cellular components of OS-sensitive proteins, and detailed molecular mobility and time-resolved PY proteomics between fluxes of OS dimers or OS Δ UD dimers..

A. GO cellular components and biological processes enriched in the list of the OS-sensitive proteins downstream of both OS+GFP-Caax and OS+CIBN-GFP-Caax activation.

B. Each proteins indicated in Fig.5E were replaced by its GO biological process. GO of each OS-sensitive proteins (or nodes) presenting only a change in the amplitude of phosphorylation between both conditions were framed, while any OS-sensitive proteins presenting a change of phosphorylation behavior between both conditions were color coded.

C. Quantification of the characteristic time of recovery after FRAP of the OS or OS Δ UD dimers (SD; N=3; 25 cells; unpaired t test) and after their activation (blue TIRF) associated with their relocation in adhesive sites. Representative time series of TIRF images during FRAP experiments achieved after OS activation (blue TIRF) and relocation to adhesive sites (white dashed line).

D. Venn diagram of PY proteins at time 0 (steady-state) shows the high homology between OS and OS Δ UD conditions. OS activation significantly affects PY enrichment of 28% (OS-sensitive proteins) of the proteins identified at time 0.

E. GO cellular components and biological processes enriched in the list of the OS-sensitive proteins in both conditions S and OS Δ UD activation.

F. Detailed fuzzy c-means clustering analysis of OS-sensitive proteins observed in MDCK cells expressing OS. Behavior for each PY protein is color coded (green) and grouped inside a cluster defined by an average trend (blue). Dynamic behaviors of these OS-sensitive proteins were grouped into 6 clusters. Comparing average curve tendencies showed high similarity between each cluster of OS and OS Δ UD conditions.

Scale bar: μm .

Table S1: List of OS-sensitive proteins, clustering analysis and prediction as potential SRC substrates downstream of either OS+GFP-Caax or OS+CIBN-GFP-Caax activations in MDCK cells.

[Click here to Download Table S1](#)

Table S2: List of OS-sensitive proteins, clustering analysis and prediction as potential SRC substrates downstream of either OS or OSAUD activations in MDCK cells.

[Click here to Download Table S2](#)

Table S3

[Click here to Download Table S3](#)

Table S4

[Click here to Download Table S4](#)



Movie 1. Local activation of OS induces a characteristic local SRC-dependent structure, a dorsal ruffle.

Representative time series (min:sec) of local activation of OS (blue square, 16 mHz) in MEF cells.



Movie 2. Light-dependent OS dimerization induces a rapid and specific OS flux targeting adhesive sites.

Representative time series (min:sec) of blue light stimulation (33 mHz) of MDCK cell expressing OS and vinculin-GFP.



Movie 3. Relocalization of OS dimers to adhesive sites is dependent on functional SRC SH3 domains.

Representative time series (min:sec) of blue light stimulation (33 mHz) of MDCK cell expressing OSΔSH3 and vinculin-GFP.



Movie 4. Membrane relocalization of activated OS dimers induces a rapid OS flux targeting adhesive sites.

Representative time series (min:sec) of blue light stimulation (33 mHz) of MDCK cell expressing OS +CIBN-GFP-Caax and vinculin-iRFP.



Movie 5. Induction of OS dimer flux into adhesive sites induces multiple and dynamic invadosome rings.

Representative time series (min:sec) of blue light stimulation (33 mHz) of MDCK cell expressing OS and LifeAct-iRFP.



Movie 6. Membrane relocalization of activated OS dimers induces characteristic large lamellipodia.

Representative time series (min:sec) of blue light stimulation (33 mHz) of MDCK cell expressing OS+CIBN-GFP-Caax and LifeAct-iRFP.